

Faster region-based convolutional neural network for plant-parasitic and non-parasitic nematode detection

Natalia Angeline¹, Nabila Husna Shabrina¹, Siwi Indarti²

¹Department of Computer Engineering, Faculty of Engineering and Informatics, Universitas Multimedia Nusantara, Tangerang, Indonesia

²Department of Crop Protection, Faculty of Agriculture, Universitas Gadjah Mada, Yogyakarta, Indonesia

Article Info

Article history:

Received Sep 21, 2022

Revised Nov 19, 2022

Accepted Nov 23, 2022

Keywords:

Faster RCNN

Nematodes

Non-parasitic

Object detection

Plant-parasitic

ABSTRACT

Nematodes represent very abundant and the largest species diversity in the world. Nematodes, which live in a soil environment, possess several functions in agricultural systems. There are two huge groups of soil nematodes, a non-parasitic nematode, which contributes positively to ecological processes, and a plant-parasitic nematode, which cause various disease and reduces yield losses in the agricultural system. Early detection and classification in the agricultural area infected with plant-parasitic nematode and interpreting the soil level condition in this area required a fast and reliable detection system. However, nematode identification is challenging and time-consuming due to their similar morphology. This study applied a pre-trained faster region-based convolutional neural network (RCNN) for plant-parasitic and non-parasitic nematodes detection. These deep learning-based object detection models gave satisfactory results as the accuracy reached 87.5%.

This is an open access article under the [CC BY-SA](https://creativecommons.org/licenses/by-sa/4.0/) license.



Corresponding Author:

Nabila Husna Shabrina

Department of Computer Engineering, Faculty of Engineering and Informatics

Universitas Multimedia Nusantara

Street of Scientia Boulevard, Tangerang, 15111, Indonesia

Email: nabila.husna@umn.ac.id

1. INTRODUCTION

The nematode family, a family of roundworms from the phylum nematoda, represents the largest species diversity in the world [1], [2]. They live in almost any environment, such as soil, water, plants, and animals [3]-[6]. Despite ubiquitous in many habitats, nematodes are often overlooked due to their small size. They are microscopic and can be as little as 250 μm or as large as 10 mm. Their diameter rarely reaches 40 μm and is typically not visible to the unaided eye [7]. Due to their tiny size and complex taxonomy, nematodes have not gotten much attention in the aquatic environment. However, they are still important in those ecosystems [5], [8].

Nematodes possess a crucial part in the soil ecosystem as essential members of the soil fauna. They participate in complicated food webs with other soil organisms to carry out important tasks and provide ecological services, such as the preservation of soil structure. Additionally, they participate in biological processes like nitrogen cycling and play important roles in soil ecology, which both have an impact on crop plants [9], [10]. There are two huge groups of soil nematodes, the first group is a beneficial nematode known as a non-parasitic nematode, and the second group is a plant-parasitic nematode. Most soil nematode species contribute positively to ecological processes rather than being plant parasites or pests. For example, the microbial community, which controls decomposition rates and affects the growth and metabolic activities of microorganisms, is influenced by microbial grazing mesofauna, such as nematodes. There are inherent

mechanisms in both of the opposing nematode groups that keep and regulate the balance of life in many creatures [11]-[13]. The other group, the plant-parasitic nematode, is a significant threat to agricultural production [14]. These groups have a primary role in causing damage and reducing yield losses. The damage caused by plant-parasitic nematodes is estimated to be up to \$US80 billion annually [15]. These plant parasitic nematodes cause various diseases that can be fatal to the infected plants.

The contradictory behavior of those two nematodes requires reliable identification. Nematodes identification is challenging due to the number of factors that may influence the performance of the identification, including their tiny size and the massive amount of diversity of nematodes present in a sample. The other reasons are the non-availability of specific morphological features and the choice of the most accurate and appropriate method [3], [16], [17]. The existing method may be a traditional one, which is time-consuming and prone to error. The improvement approach is necessary for nematode identification. A fast and accurate detection and classification system of those two groups of nematodes was required in the early diagnosis of the infectious plant and soil fertility level. The soil sample containing more parasitic nematodes indicates the plant was contaminated with plant-parasitic nematodes. In contrast, a more significant number of non-parasitic nematodes represent healthy and fertile soil.

Deep learning could be an alternative to support nematode identification reliably and more quickly. Convolutional neural networks (CNNs) based methods were already implemented in previous studies for nematode identification. Abade *et al.* [18] proposed a new CNN model named NemaNet for Brazil's nematode soybean crop identification. The proposed method gave the accuracy up to 96.99%. A novel end-to-end deep convolutional selective autoencoder (DSCA) for identifying and counting soybeans ceast nematode egg was done by [19]. The method gave satisfactory results and made the identification process faster. Nemarec, a deep learning-based web application for the nematode identification process, was proposed by [20], [21]. They use their self-collected dataset for the research. The result showed that the model could adequately identify 94-97% of the nematode when applied data augmentation. Uhlemann *et al.* [22] explored using CNN models for entomopathogenic nematode identification. This research discovered that optimal hyperparameters and fine-tuning could help improve the performance of the identification process. Deep learning-based object detection models for juvenile stages nematode detection were demonstrated by [23]. This research proposed a faster region-based convolutional neural network (RCNN) with scale aware (SA) approach for detecting and identifying microscopic images of nematodes.

CNN-based methods are already proven can help speed up nematode identification. However, the previous research may not be applicable in a different area as the species and characteristics of each nematode are not identic. This study will conduct detection and classification for plant-parasitic and non-parasitic nematodes commonly found in Indonesia, as the species frequently found in Indonesia are not covered in the previous study. We build an additional small image dataset for plant-parasitic and non-parasitic nematodes in Indonesia. The nematodes dataset represents the images captured from the real-world data and reflects the challenges faced by real-world constraints. Faster RCNN was implemented for this application as it is suitable for dealing with small datasets [24]. Data augmentation was also applied to increase the data variation and prevent overfitting [25].

2. METHOD

Figure 1 shows the complete workflow for plant-parasitic and non-parasitic nematode detection. Initially, the data collection was performed by collecting the nematode pictures taken in Central Java, Indonesia. The collected dataset is then preprocessed using image resized by changing the image size to 416 x 416 to fit the input size of the deep learning model. To increase the size of the datasets, augmentation methods, such as brightness, exposure, rotation, flip, and shear, were also applied in the image preprocessing steps. The Faster RCNN with ResNet101 backbone model was then built and trained using the processed datasets. The model's performance result was then evaluated using several metrics, such as average precision, average recall, and accuracy. More detailed explanations are described in the following sub-sections.

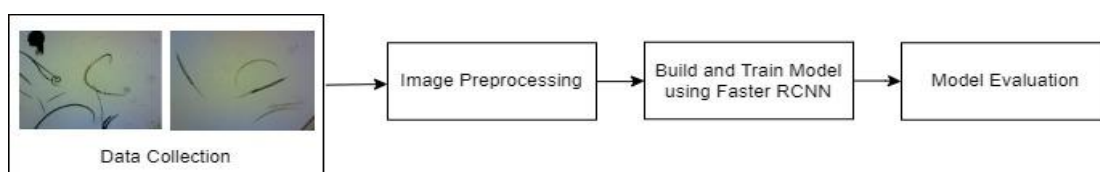


Figure 1. Research workflow

2.1. Nematode datasets

The datasets were collected in agricultural lands in Central Java, Indonesia. The soil was collected at a depth of 5-30 cm. The nematodes were then isolated and extracted from the soil sample using the Whitehead tray method with modification referred to [26]. Each soil sample was gently homogenized using a hand mixer, and stones were manually removed. Nematodes were placed on a tray and added with water until they covered all soil using 100 grams of soil. The nematode moving toward the water was gathered on the tubes for further morphological identification and classification. Each group of nematodes was observed using a light microscope Olympus CX31 with a magnification of 40-1,000 [27]. In detail, nematode identification was made based on the mouth part of the nematode, as explained and referred to [28]. The datasets represent the nematodes commonly found in Indonesia and are classified into two groups, non-parasitics, and plant-parasitic. Figure 2 shows the sample of the nematode dataset. Figures 2(a) and 2(b) show the microscopic image sample of non-parasitic and plant parasitic nematodes, respectively. As seen in the example, both classes' morphology is hard to distinguish using the unaided eye. Figure 2(c) shows the sample of mixed nematodes, consisting of non-parasitic and plant-parasitic extracted from the same soil sample.

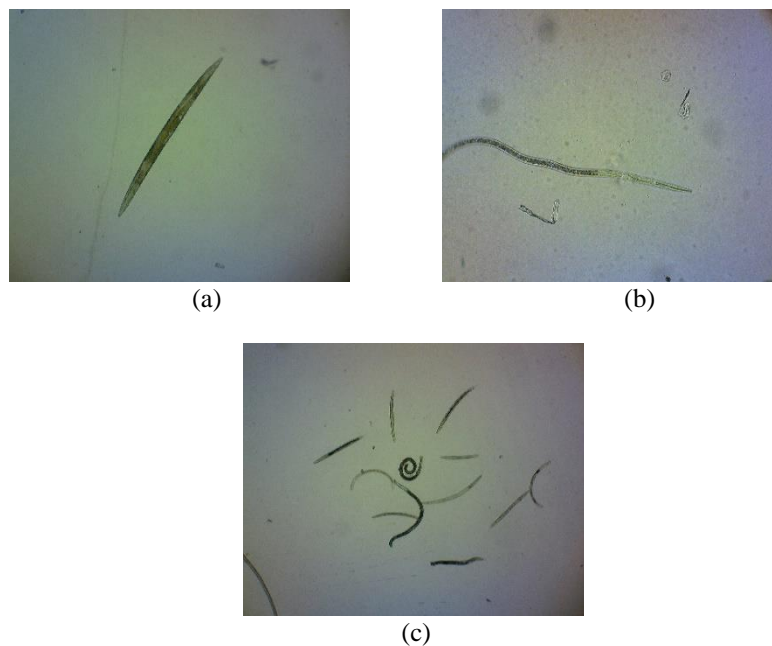


Figure 2. Sample of nematodes dataset (a) sample of non-parasitic nematode, (b) sample of plant-parasitic nematode, and (c) sample of mix nematodes

2.2. Data preprocessing

The collected data were then preprocessed using resize to fit the model's input. Annotation and augmentation were then implemented using roboflow software [29] to enlarge the size of the datasets. The datasets applied augmentation, such as brightness, rotation, flip, exposure, and shear. There are 1,625 augmented images of nematodes used in this study, divided into 1415 images for the training dataset and 210 images for the testing dataset. The images were then annotated and labeled, resulting in 3,550 plant-parasitic nematodes and 3,733 non-parasitic nematodes. The sample of annotated and augmented nematodes image can be seen in Figure 3 and Figure 4, respectively.

Figure 4(a) shows a comparison of brightness augmentation with the original image, where the augmentation results in a brighter image. Figure 4(b) presents the result of shear augmentation. The shear can affect the performance of the model because the shape of the nematodes can change, such as being cut off or causing the bounding boxes to overlap. Figure 4(c) presents a comparison of exposure augmentation with the original image. Where brightness affects the overall darkness of the image, exposure will only transform on the object's highlight. Figure 4(d) shows a comparison of the flip augmentation with the original image. Flips can be done both vertical and horizontal. Figure 4(e) presents the result of rotate augmentation, which is applied by rotating the image by 90 degrees. Both flip and rotate augmentation can affect model performance because it changes the positional characteristics of the nematodes.



Figure 3. Sample of annotated and labelled image

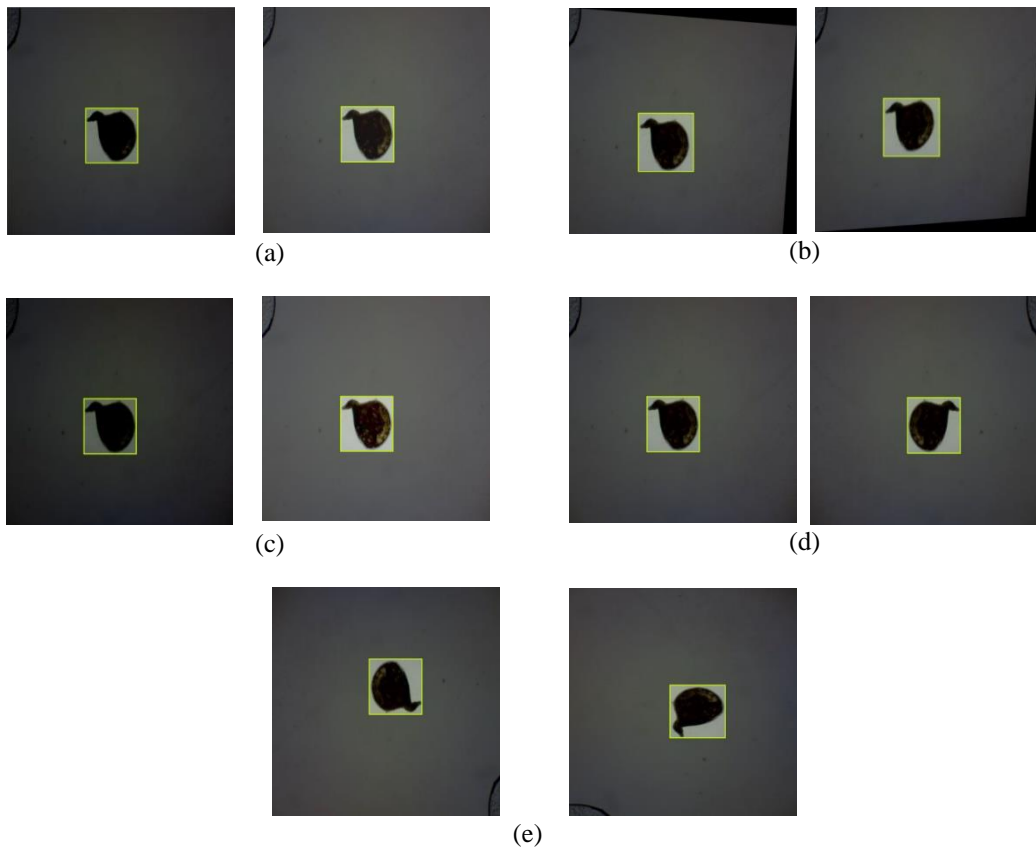


Figure 4. Sample of augmented image (a) brightness, (b) shear, (c) exposure, (d) flip, and (e) rotation

2.3. Faster RCNN architecture

Nematode detection and classification are performed using faster RCNN with ResNet101 backbone. Faster RCNN was chosen based on its best performance in a small dataset, compared to single shot detection (SSD) and you only look once (YOLO) V3 [24]. Faster RCNN consists of two modules, to propose a region, called as a deep-fully convolutional network and the fast R-CNN detector [30] to detect the object using the proposed region [31]. Figure 5 and Figure 6 present the diagram of the faster RCNN with ResNet101 backbone applied in this study. Initially, in region proposal network (RPN), a feature extractor process an image using ResNet101. At a chosen intermediate level, the selected features are then used to forecast class box proposals.

These box proposals are used to crop features from the same intermediate feature map in the second stage, which is then supplied to the remaining feature extractor to predict a class and class-specific box refinement for each proposal.

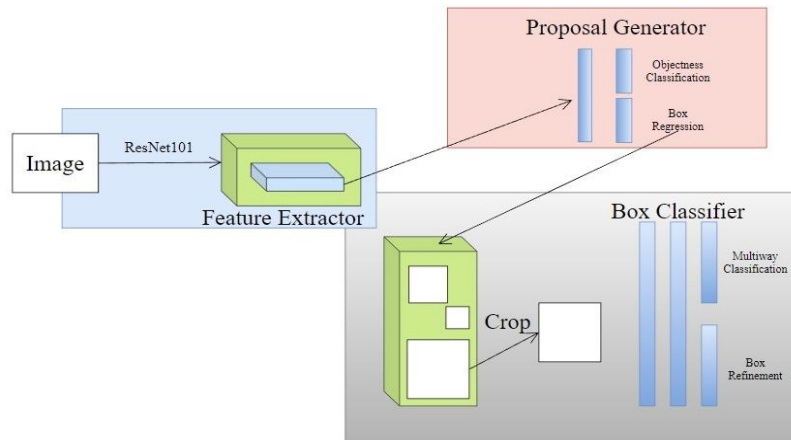


Figure 5. Faster R-CNN with ResNet101 as feature extractor

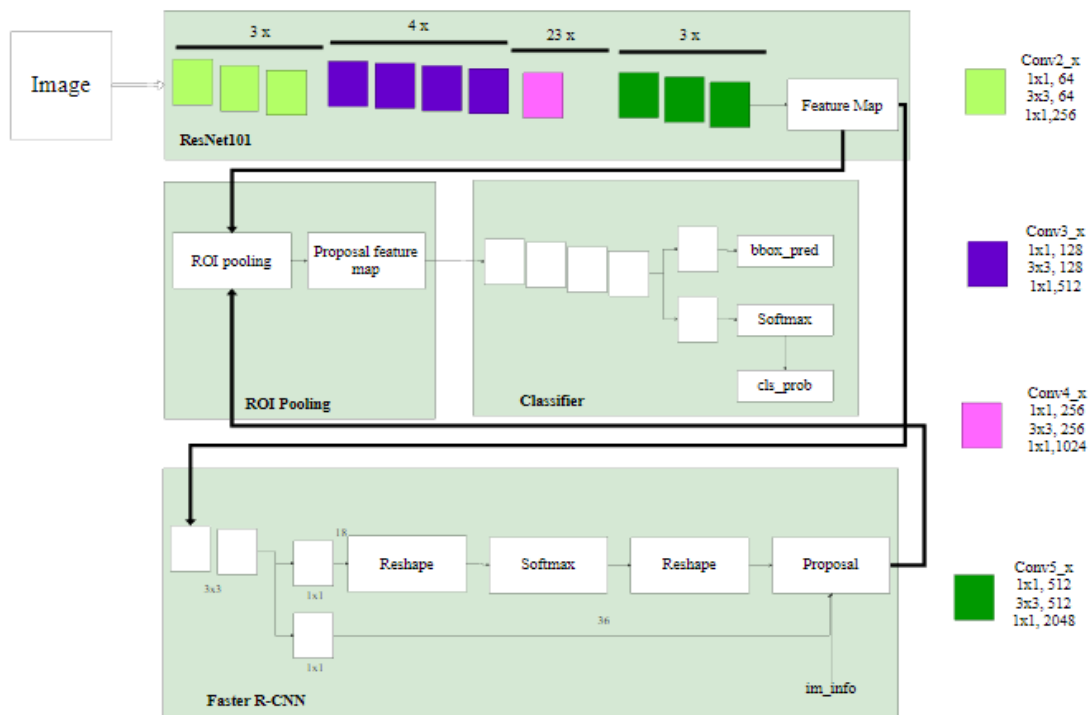


Figure 6. Faster RCNN with ResNet 101 architecture

Figure 6 shows the full architecture of faster RCNN with ResNet 101 backbone. The features were extracted using a ResNet-101 that had been pre-trained on the ImageNet dataset. Then, a bounding box was created using a region proposal network. The suggestion box was also mapped to the feature map of the convolutional neural network's final layer. The region of interest pooling layer produces a fixed-size feature map. Finally, utilizing softmax loss, joint training of classification probabilities and border regressions was implemented.

The model works when it receives an input image of a specific size. The image is then processed by four convolution layers with a kernel description of each layer and a total of 101 convolution layers. The feature map obtained is then used to find the region of interest (ROI) or object in the image. ROI is also obtained from

the network proposal region that accepts the feature map as input to predict the bounding box in the image. Then, both results will be pooled and given to a fully connected layer to get the bounding box prediction along with the classification results of each predicted bounding box.

2.4. Evaluation metric

As the dataset is considered balanced, and the predicted class is equally important, instead of the predicted score, the accuracy metric was selected [32]. Accuracy is applied to measure the model's overall average accuracy through all images in the test set. Other metrics used in this study are average precision and average recall. Average precision is based on the region beneath a precision and recall curve after removing the zig-zag behavior during pre-processing. It provides an overview of the precision-recall trade-off generated by the confidence intervals for the expected bounding box [33]. The average recall is used to assess the assertiveness of object detectors for a specific class [34]. While calculating average precision and average recall, precision and recall concepts were used, defined as in (1) and (2).

$$Precision (P) = \frac{TP}{TP+FP} \quad (1)$$

$$Recall (R) = \frac{TP}{TP+FN} \quad (2)$$

Where TP – True Positive; FP – False Positive; TN – True Negative; FN – False Negative. The for accuracy is given in (3), and for Average Precision is presented in (4)-(5).

$$Test Accuracy = \frac{TP+TN}{TP+TN+FP+FN} \quad (3)$$

$$Average Precision = \frac{1}{11} \sum_{R \in \{0.0, \dots, 1.0\}} P_{interp}(R) \quad (4)$$

$$P_{interp}(R) = \max_{\tilde{r} \geq r} P(\tilde{R}) \quad (5)$$

The average recall is the highest recall value at a set number of detections per image averaged over IOUs and classes, with the in (6).

$$Average Recall = 2 \int_{0.5}^1 recall(IoU) dIoU \quad (6)$$

IoU is Intersection over Union, which measures the ratio between the area of overlap and the area of union between the predicted bounding box and the ground truth bounding box.

2.5. System implementation

The model was trained using Google Colab Notebook (Free Version) [35], with specifications of Nvidia K80/T4 GPU, a memory of 12GB/16GB, CPU 2-core Xeon 2.2GHz, and 12 GB RAM, which can be used based on availability. TensorFlow and Keras library, with fully built and pre-trained Faster RCNN with ResNet101 backbone model, was used for code implementation. The model was then trained using the transfer learning method. SGD optimizer with momentum [36] was applied in this research. The configuration consisting of a batch size 64 and learning rate of 0.04 were carried out.

3. RESULTS AND DISCUSSION

The sample result of plant-parasitic and non-parasitic nematode detection using Faster RCNN ResNet 101 are presented in Figure 7 and Figure 8. Figure 7 shows that the model can correctly detect 13 parasites from a total of 14 parasites in the picture, with the undetected nematode marked with the red box. The detection confidence score reached 100%, with the lowest confidence level being 75%. The undetected parasite nematode was due to the overlapping position of the bounding box, which caused a decrease in detection and classification performance. Figure 8 shows the detection result on an image with the plant-parasitic and non-parasitic nematode. The model can detect all nematodes; however, there is one error misclassification of parasite nematode, which is marked with the red box. The misclassification may occur due to the similar features between plant-parasitic and non-parasitic nematodes. Nevertheless, the model's confidence score reached 100%, with the lowest confidence score of 86%.

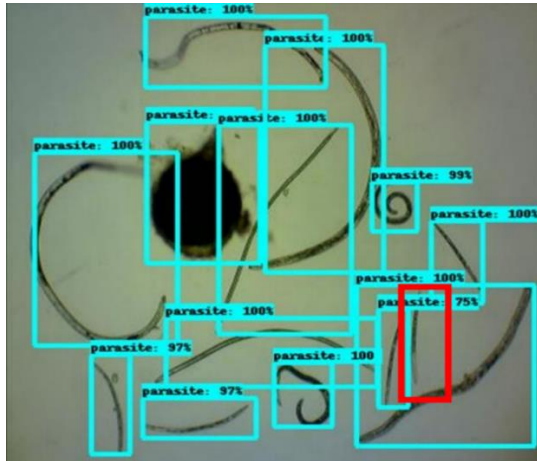


Figure 7. Sample result of plant-parasitic nematode detection

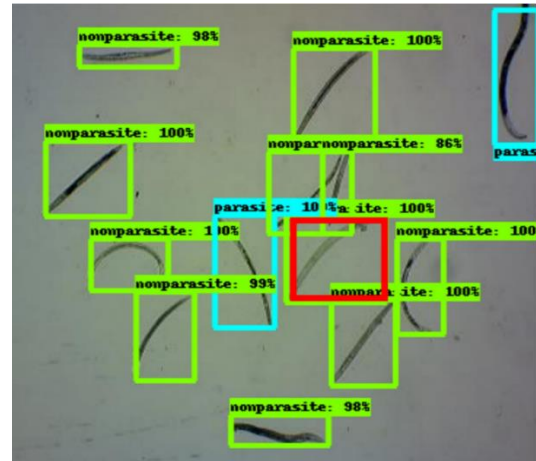


Figure 8. Sample result of plant-parasitic and non-parasitic nematode detection

The model was trained using single augmentation such as brightness, exposure, flip, shear, and rotation in the experimental setup. This training was carried out to find the three best augmentations that giving the best performance. The result in Table 1 shows that the nematode dataset augmented using brightness, rotate 90, shear, and exposure was performing better than the original dataset. However, the flip resulted in worse performance with average precision and an average recall of 0.473 and 0.617, respectively. The model performance declined when there were more data with different orientations due to the relatively small dataset. Moreover, flip augmentation caused the model could not differentiate the data based on different orientations.

The best performance occurred when the model applied brightness augmentation. The highest average precision and average recall were 0.53 and 0.678, respectively. Both highest versions were a result of the model trained using brightness augmentation. Based on the result in Table 1, the best three performances are model applied brightness, rotate 90, and shear augmentation.

The best three augmentation method was combined to perform double and triple augmentation on the nematode dataset. In experimental results, the best augmentation is obtained from brightness augmentation. Therefore, the model will be applied brightness augmentation with two other augmentations. Brightness augmentation will also be combined in the triple combination, along with 90 degrees of rotation and shear. The result of the faster RCNN ResNet101 with various combinations of augmentation was given in Table 2.

Table 1. Experimental setup results using single augmentation

Dataset	Metric performance	
	Average precision	Average recall
Original	0.501	0.644
Brightness	0.530	0.678
Exposure	0.510	0.623
Flip	0.473	0.617
Shear	0.514	0.629
Rotate 90	0.517	0.665

Table 2. Faster RCNN ResNet101 results with augmenattions

Dataset	Metric performance		
	Average precision	Average recall	Accuracy
Original	0,611	0,733	0,68852
Brightness	0,712	0,793	0,78947
Brightness, Rotate 90	0,725	0,808	0,83930
Brightness, Shear	0,619	0,709	0,84483
Brightness, Rotate 90, Shear	0,613	0,685	0,87500

The result in Table 2 shows that a combination of augmentation positively impacts model performance compared to performance on the original dataset and single augmentation. When trained using augmented nematode datasets, the faster RCNN ResNet101 results in 78.94% up to 87.5% accuracy. The minimum and maximum average precision are 0.613 and 0.725, respectively. The best average precision resulted from the

model trained using a combination of brightness and 90 degrees of rotation augmentations. The average recall of the model trained using data augmentation ranged from 0.685 up to 0.808. The highest average recall score also occurred when the model applied a combination of brightness and rotated 90 augmentations. With an accuracy of 87.5%, this research outperformed similar previous research in [23].

4. CONCLUSION

The faster RCNN ResNet101 model is a promising method for detecting plant-parasitic and non-parasitic nematodes. The model gives the highest accuracy reaching up to 87.5%. This work demonstrated the capability of using a deep learning-based object detection model to detect and classify plant-parasitic and non-parasitic nematodes commonly found in Indonesian soil. The applied augmentation method improved model performance compared to the original nematode dataset. The dataset implemented with a combination of brightness, rotate 90, and shear augmentation resulted in the best accuracy of 87.5%. The best average precision and average recall score occurred when the model implemented a combination of brightness and rotated 90 augmentations. Further work is still needed to improve model performance detecting and classifying plant-parasitic and non-parasitic nematodes. Future work will focus on: a) Investigate other deep learning-based object detection models, such as YOLO, to improve the performance of detection systems for plant-parasitic and non-parasitic nematodes, b) Further development of the nematodes' dataset.

ACKNOWLEDGEMENTS

We would like to acknowledge the supports given by Universitas Multimedia Nusantara during this study. We would also like to thank Rina Maharani, S.P., M.Sc who help us to collect and prepare nematodes dataset.




REFERENCES

- [1] J. V. D. Hoogen *et al.*, "Soil nematode abundance and functional group composition at a global scale," *Nature*, vol. 572, no. 7768, pp. 194–198, Aug. 2019, doi: 10.1038/s41586-019-1418-6.
- [2] T. Bongers and M. Bongers, "Functional diversity of nematodes," *Applied Soil Ecology*, vol. 10, no. 3, pp. 239–251, Nov. 1998, doi: 10.1016/S0929-1393(98)00123-1.
- [3] Y. Seesao, M. Gay, S. Merlin, E. Viscogliosi, C. M. Aliouat-Denis, and C. Audebert, "A review of methods for nematode identification," *J Microbiol Methods*, vol. 138, pp. 37–49, Jul. 2017, doi: 10.1016/j.mimet.2016.05.030.
- [4] O. Holovachov, "Nematodes from terrestrial and freshwater habitats in the arctic," *Biodivers Data J*, vol. 2, p. e1165, Aug. 2014, doi: 10.3897/BDJ.2.e1165.
- [5] C. Ptatscheck and W. Traunspurger, "The ability to get everywhere: dispersal modes of free-living, aquatic nematodes," *Hydrobiologia*, vol. 847, no. 17, pp. 3519–3547, Oct. 2020, doi: 10.1007/s10750-020-04373-0.
- [6] A. Kergunteuil, R. Campos-Herrera, S. Sánchez-Moreno, P. Vittoz, and S. Rasmann, "The abundance, diversity, and metabolic footprint of soil nematodes is highest in high elevation alpine grasslands," *Front Ecol Evol*, vol. 4, Jul. 2016, doi: 10.3389/fevo.2016.00084.
- [7] A. Swart, M. Marais, C. Mouton, and G. C. du Preez, "Non-parasitic, terrestrial and aquatic nematodes," in *Nematology in South Africa: A View from the 21st Century*, Cham: Springer International Publishing, 2017, pp. 419–449, doi: 10.1007/978-3-319-44210-5_20.
- [8] W. K. Dodds, "Animals," in *Freshwater Ecology*, Elsevier, 2002, pp. 152–180, doi: 10.1016/B978-012219135-0/50010-6.
- [9] A. Ridall and J. Ingels, "Suitability of free-living marine nematodes as bioindicators: Status and future considerations," *Front Mar Sci*, vol. 8, Jul. 2021, doi: 10.3389/fmars.2021.685327.
- [10] G. S. Moura and G. Franzener, "Biodiversity of nematodes biological indicators of soil quality in the agroecosystems," *Arq Inst Biol (Sao Paulo)*, vol. 84, no. 0, Nov. 2017, doi: 10.1590/1808-1657000142015.
- [11] D. A. Neher, "Role of nematodes in soil health and their use as indicators," *J Nematol*, vol. 33, no. 4, pp. 161–8, Dec. 2001.
- [12] D. A. Neher, "Ecology of plant and free-living nematodes in natural and agricultural soil," *Annu Rev Phytopathol*, vol. 48, no. 1, pp. 371–394, Jul. 2010, doi: 10.1146/annurev-phyto-073009-114439.
- [13] G. D. Preez *et al.*, "Nematode-based indices in soil ecology: Application, utility, and future directions," *Soil Biol Biochem*, vol. 169, p. 108640, Jun. 2022, doi: 10.1016/j.soilbio.2022.108640.
- [14] J. Poveda, P. Abril-Urias, and C. Escobar, "Biological control of plant-parasitic nematodes by filamentous fungi inducers of resistance: Trichoderma, mycorrhizal and endophytic fungi," *Front Microbiol*, vol. 11, May 2020, doi: 10.3389/fmicb.2020.00992.
- [15] J. T. Jones *et al.*, "Top 10 plant-parasitic nematodes in molecular plant pathology," *Mol Plant Pathol*, vol. 14, no. 9, pp. 946–961, Dec. 2013, doi: 10.1111/mpp.12057.
- [16] M. Bogale, A. Baniya, and P. DiGennaro, "Nematode identification techniques and recent advances," *Plants*, vol. 9, no. 10, p. 1260, Sep. 2020, doi: 10.3390/plants9101260.
- [17] C. M. Bredtmann, J. Krücken, J. Murugaiyan, T. Kuzmina, and G. V. Samson-Himmelstjerna, "Nematode species identification—current status, challenges and future perspectives for cyathostomins," *Front Cell Infect Microbiol*, vol. 7, Jun. 2017, doi: 10.3389/fcimb.2017.00283.
- [18] A. Abade, L. F. Porto, P. A. Ferreira, and F. D. B. Vidal, "NemaNet: A convolutional neural network model for identification of soybean nematodes," *Biosyst Eng*, vol. 213, pp. 39–62, Jan. 2022, doi: 10.1016/j.biosystemseng.2021.11.016.
- [19] A. Akintayo, G. L. Tylka, A. K. Singh, B. Ganapathysubramanian, A. Singh, and S. Sarkar, "A deep learning framework to discern and count microscopic nematode eggs," *Sci Rep*, vol. 8, no. 1, p. 9145, Dec. 2018, doi: 10.1038/s41598-018-27272-w.
- [20] X. Qing *et al.*, "NemaRec: A deep learning-based web application for nematode image identification and ecological indices calculation," *Eur J Soil Biol*, vol. 110, p. 103408, May 2022, doi: 10.1016/j.ejsobi.2022.103408.




- [21] X. Lu, Y. Wang, S. Fung, and X. Qing, "I-Nema: A biological image dataset for nematode recognition," *arXiv preprint arXiv:2103.08335*, Mar. 2021.
- [22] J. Uhlemann, O. Cawley, and T. Kakouli-Duarte, "Nematode identification using artificial neural networks," in *Proceedings of the 1st International Conference on Deep Learning Theory and Applications*, 2020, pp. 13–22, doi: 10.5220/0009776600130022.
- [23] J. Lu, H. Qiu, W. Xu, and Z. Zhao, "Deep learning for nematode detection and classification," <https://basproject-2018spring.github.io/Website/> (accessed Apr. 01, 2022).
- [24] S. Srivastava, A. V. Divekar, C. Anilkumar, I. Naik, V. Kulkarni, and V. Pattabiraman, "Comparative analysis of deep learning image detection algorithms," *J Big Data*, vol. 8, no. 1, p. 66, Dec. 2021, doi: 10.1186/s40537-021-00434-w.
- [25] C. Shorten and T. M. Khoshgoftaar, "A survey on image data augmentation for deep learning," *J Big Data*, vol. 6, no. 1, p. 60, Dec. 2019, doi: 10.1186/s40537-019-0197-0.
- [26] J. Southey, *Laboratory Methods for Work with Plant and Soil Nematodes*. London: Her Majesty's Stationary Office, 1986.
- [27] S. Indarti, A. Soffan, and M. M. F. Andrasmaria, "Short communication: first record of hirschmanniella mucronata (Nematoda: Pratylenchidae) in Yogyakarta, Indonesia," *Biodiversitas*, vol. 21, no. 5, Apr. 2020, doi: 10.13057/biodiv/d210533.
- [28] J. Heyns, *A guide to the plant and soil nematodes of South Africa*. Cape Town: Balkema (A.A.), 1971.
- [29] Roboflow, "Roboflow software," <https://roboflow.com/annotate> (accessed Apr. 01, 2022).
- [30] R. Girshick, "Fast R-CNN," in *2015 IEEE International Conference on Computer Vision (ICCV)*, Dec. 2015, pp. 1440–1448, doi: 10.1109/ICCV.2015.169.
- [31] S. Ren, K. He, R. Girshick, and J. Sun, "Faster R-CNN: Towards real-time object detection with region proposal networks," *IEEE Trans Pattern Anal Mach Intell*, vol. 39, no. 6, pp. 1137–1149, Jun. 2017, doi: 10.1109/TPAMI.2016.2577031.
- [32] R. Padilla, S. L. Netto, and E. A. B. D. Silva, "A survey on performance metrics for object-detection algorithms," in *2020 International Conference on Systems, Signals and Image Processing (IWSSIP)*, 2020, pp. 237–242, doi: 10.1109/IWSSIP48289.2020.9145130.
- [33] R. Padilla, W. L. Passos, T. L. B. Dias, S. L. Netto, and E. A. B. D. Silva, "A comparative analysis of object detection metrics with a companion open-source toolkit," *Electronics (Basel)*, vol. 10, no. 3, p. 279, Jan. 2021, doi: 10.3390/electronics10030279.
- [34] K. Oksuz, B. C. Cam, E. Akbas, and S. Kalkan, "Localization recall precision (LRP): A new performance metric for object detection," in *Proceedings of the European Conference on Computer Vision (ECCV)*, 2018, pp. 521–537, doi: 10.1007/978-3-030-01234-2_31.
- [35] Google, "Welcome to Colab!," *google.com*. <https://colab.research.google.com/> (accessed Apr. 01, 2022).
- [36] P. Zhou, J. Feng, C. Ma, C. Xiong, S. Hoi, and W. E., "Towards theoretically understanding why SGD generalizes better than adam in deep learning," *Advances in Neural Information Processing Systems*, vol. 33, pp. 21285–21296, Oct. 2020.

BIOGRAPHIES OF AUTHORS






Natalia Angeline    is currently a Bachelor of Computer Engineering in Universitas Multimedia Nusantara. Her interest includes data science, image processing, and ERP systems. She can be contacted at email: via.nataliaangeline29@gmail.com.



Nabila Husna Shabrina    received her bachelor's degree in telecommunication engineering and master's degree in electrical engineering from Institut Teknologi Bandung. She is currently a lecturer in Computer Engineering at Universitas Multimedia Nusantara. Her research interests include signal processing, image processing, and computer vision. She can be contacted at email: nabila.husna@umn.ac.id.



Siwi Indarti    earned her undergraduate degree from the Department of Plant Protection at the Faculty of Agriculture at Universitas Gadjah Mada. She earned a Master's and a Doctorate from the same department. She currently works at the Department of Crop Protection at Gadjah Mada University. Siwi is a lecturer and researcher in plant nematology. She has written many papers on the subject and is well-known in the field. Her longstanding interest in identifying and controlling plant parasitic nematode has led her to focus her research on this topic in recent years. She can be contacted at email: siwi.indarti@ugm.ac.id.